Study of gas ageing effect on detector performance for the development of a new gas system for ACTAR-TPC at GANIL

K. Rojeeta Devi, J. Pancin, C. Nicolle, T. Roger, M. Fisichella

▶ **To cite this version:**

K. Rojeeta Devi, J. Pancin, C. Nicolle, T. Roger, M. Fisichella. Study of gas ageing effect on detector performance for the development of a new gas system for ACTAR-TPC at GANIL. Nuclear Instruments and Methods in Physics Research Section A: Accelerators, Spectrometers, Detectors and Associated Equipment, 2024, 1069, pp.169866. 10.1016/j.nima.2024.169866 . hal-04694820

HAL Id: hal-04694820
https://hal.science/hal-04694820v1

Submitted on 11 Sep 2024

HAL is a multi-disciplinary open access archive for the deposit and dissemination of scientific research documents, whether they are published or not. The documents may come from teaching and research institutions in France or abroad, or from public or private research centers.

L'archive ouverte pluridisciplinaire **HAL**, est destinée au dépôt et à la diffusion de documents scientifiques de niveau recherche, publiés ou non, émanant des établissements d'enseignement et de recherche français ou étrangers, des laboratoires publics ou privés.

Study of gas ageing effect on detector performance for the development of a new gas system for ACTAR-TPC at GANIL

K. Rojeeta Devi[a,*], J. Pancin[a], C. Nicolle[a], T. Roger[a], M. Fisichella[a]

[a]*Grand Accélérateur National d'Ions Lourds, CEA/DRF-CNRS/IN2P3, B.P. 55027, Caen, , Cedex, France*

Abstract

Aiming to develop an advanced gas system for ACTAR-TPC (ACtive TARget and Time Projection Chamber), an extensive and detailed study was conducted to examine the effect of gas ageing on detector performance. Efficiency of gas-filters was analyzed to assess their suitability for integration into a gas system for gas recycling purpose. This paper reports the experimental methodologies employed, key data analysis methods, and the results of the study.

Keywords: Gas ageing, gas-filter, gas recycling, ACTAR-TPC

1. Introduction

ACTAR-TPC [1, 2] at GANIL (Grand Accélérateur National d'Ions Lourds) is a novel detector which works on the principle of gas-filled time projection chamber. An important characteristic of the detector is that its gas volume can also serves as a target for nuclear reactions (i.e active target). In experiments with low intensity radioactive ion beams, such active target detector fulfills the requirement of thick target (large target volume) to achieve high reaction yield without deteriorating the energy resolution. ACTAR-TPC with its integrated GET electronics [3] provides the requisites (large dynamic range, short dead time, timing measurement, multiple track records, etc) to explore structures and decays of exotic nuclei [4]. Therefore, with ACTAR-TPC, it is possible to study nuclei near the drip line and the associated phenomena which can address fascinating results in nuclear structure, reaction and astrophysics studies.

Gas purity is a key factor in ensuring optimal detector performance. However, in gas filled detectors, impurities accumulate inside the detector volume because of continuous irradiation and electron avalanches during the experiment or due to outgassing and leakages from the detector system. The accumulated impurities influence detector performance deteriorating the gain and the energy resolution. They can also reduce the detector's life span by causing harmful reactions inside the detector volume. Such undesirable effects are generally called gas ageing effect. Commonly, N_2 , O_2 and H_2O molecules accumulate due to leakages and outgassing. The presence of other impurities depends on the gas used, its purity, and the materials utilized in the mechanical set-up of the detector within the chamber. So far, ACTAR-TPC worked in continuous circulation mode to reduce possible gas ageing effects, with fresh gas delivered by a gas system unit and venting the used gas to atmosphere. Mainly, $i C_4H_{10}$, H_2, D_2 and ^{4}He gases have been used, mixed eventually with small percentages of quenchers (like $i C_4H_{10}$, CF_4, CO_2, etc) to improve the detector gain. Recently, a project has been accepted to cope ACTAR-TPC with ^{3}He gas to perform (^{3}He,d) and (^{3}He,p) transfer reactions, which are of great interest for nuclear physics. As an example, the one proton-transfer reaction (^{3}He,d) is particularly well suited to study mirror symmetry breaking in proton rich nuclei [5]. ^{25}P is one of the key candidates to show this symmetry breaking . The ^{24}Si(^{3}He,d)^{25}P reaction could provide position and width of the resonances in ^{25}P, the information on the momentum transferred and thus on the spin of the populated resonances. The use of an active target is mandatory to detect the low energy recoiling deuterons. Due to the cost and scarcity of ^{3}He, the ACTAR-TPC demonstrator (30 cm×25 cm×21 cm) will be used for this kind of experiment, and a development of a recirculation and purification gas system is essential to reduce the gas waste. Systems for gas recycling and purification have been already developed for experiments which use greenhouse gases (GHG) like CF_4, C_3F_8, because of the constraint in the release of these GHG in the atmosphere. They recycle the gas using gas-filter or gas-purification component and then re-injecting it into the

*Corresponding author

Email address: rojee29@gmail.com (K. Rojeeta Devi)

detection chamber [6, 7]. The works reported in literature concern mainly gas at pressure above the atmospheric one. In the present work, this kind of system has been developed and tested for gas pressure lower than the atmospheric one. This R&D was performed by using a longitudinal TPC equipped with a multiwires amplification gap (Mayaito [8]), available at GANIL, filled with iC$_4$H$_{10}$ gas at 85 mbar. The gas ageing effects were studied by measuring the energy and the stopping point of α-particles emitted by a ^{241}Am source as a function of time. Two different close-loop gas systems were studied, with and without filter and compared with the case of gas static mode configuration. In Section 2, the used experimental set-up is described. The data analysis methodology is reported in Section 3. Section 4 and 5 are dedicated to the study of dependence of the detector response on temperature and the associated corrections. Section 6 presents the results and the discussions concerning the ageing effects in different gas conditions. Finally, Section 7 summarizes the main conclusions.

2. Experimental description

2.1. Detector set-up

For the present study, a cylindrical chamber of $\approx$ 20 liters volume with Mayaito detector was coupled with a gas system. Mayaito is a cuboidal detection device which is composed of a cathode plate at the top, pad plane at the bottom, anode wires plane at $\approx$ 2 mm above the pad plane, and Frisch's grid in between the cathode plate and the anode wires plane at a distance of $\approx$ 2 mm from the anode wires plane. The pad plane is divided into 128 pads of 1.5 mm$\times$15 mm having 0.1 mm of inter-strip. Therefore, each pad has a depth of 1.5 mm along the α-track. Eight Gassiplex [9] ASIC's (16-channel) are connected to the back of the pad plane for signals reading from the 128 pads. A schematic representation of the detector set-up is shown in Figure 1. ^{241}Am source is placed at the side wall of Mayaito with a collimator of length $\approx$ 33 mm and diameter $\approx$ 5 mm. There is a dead zone of $\approx$ 38 mm between the α-source and the active area of the detector. A temperature measurement unit using PT100 sensor is also installed to monitor the temperature variation during a run period.

The detector was filled with iC$_4$H$_{10}$ gas at $\approx$ 85 mbar pressure. Pressure of the gas was optimized in such a way that the α-particles lost all their energy (5486 keV) within the active volume of the detector and stop inside it. Interaction of the incident α-particles with the gas atoms/molecules will generate ionization electrons. Operating voltages of $-$800 V and 600 V, optimized for good gain and energy resolution, are applied to the cathode and the anode respectively. The Frisch's grid and the pad plane are kept at ground potential. The vertical electric field created between the cathode and the Frisch's grid will force the ionization electrons to move towards the amplification zone, between the Frisch's grid and the anode wires plane.

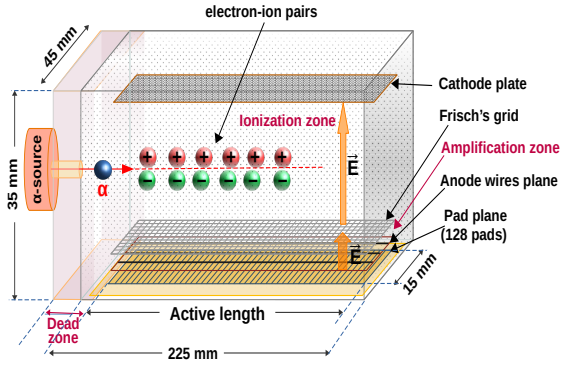

Figure 1: Schematic of the detector set-up (not to scale).

In the amplification zone, the ionization electrons are amplified by creating electron avalanches. This induces a charge deposition in each pad proportional to the energy deposited by the α-particle along its track. The charge signals are read out through the Gassiplex chips which generate multiplexed signals and are sent to the data acquisition circuit. The signal conversion for data acquisition is done by using NUMEXO2, a digitizer module developed at GANIL.

2.2. Gas system

In Figure 2, a schematic of the gas system coupled with the detector chamber is shown. The gas system can deliver different gases to the detector chamber by setting a chosen pressure and flow rate. It can be operated in two different modes which are referred as "static mode" and "circulation mode". In the static mode, the chamber is filled with a selected gas at a set pressure. In the circulation mode, gas supply inside the chamber is done by continuous circulation of gas, regulating a set pressure through three different sub-modes which are as follows:

1. Open-loop circulation: The chamber is circulated with fresh gas. Gas exiting from the chamber is either released in the atmosphere or is collected to a collection gas bottle through the exhaust line.
2. Close-loop circulation without filter: For the circulation, gas exiting from the chamber is sent back to the chamber without any prior cleaning.

3. Close-loop circulation with filter: Gas exiting from the chamber is cleaned by passing through a gas-filter unit and the cleaned-gas is sent back to the chamber for circulation.

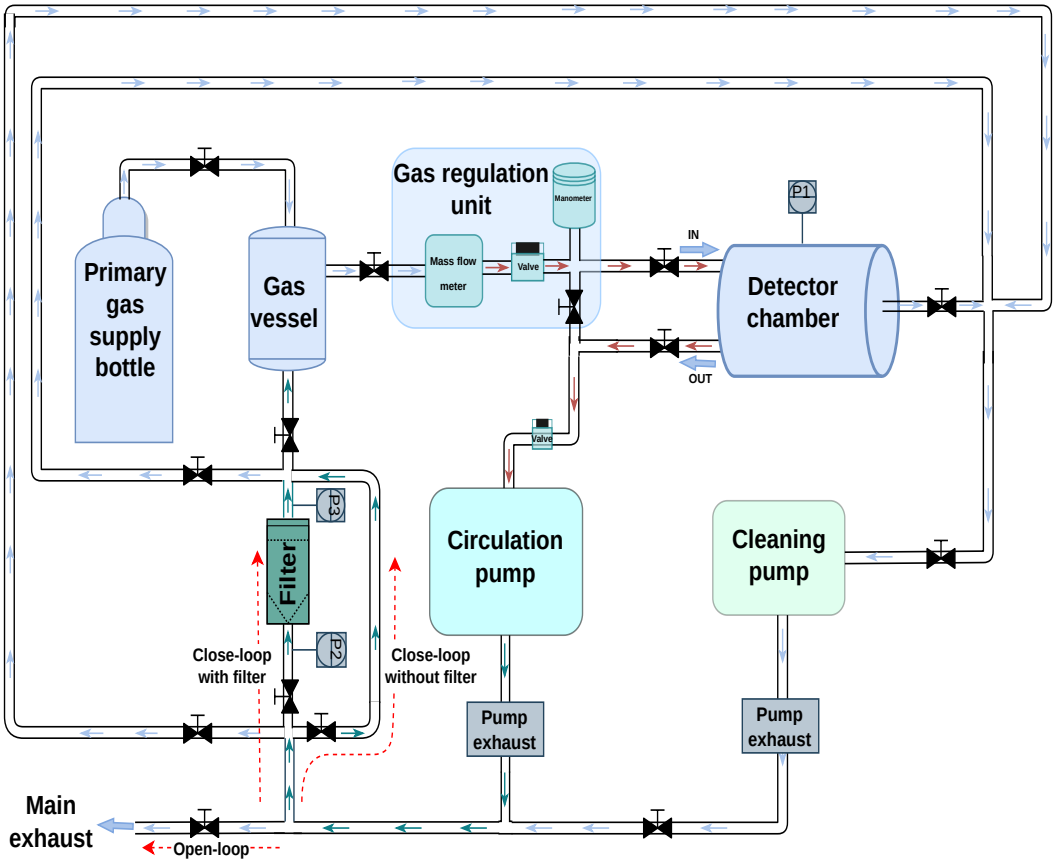

Figure 2: Gas system coupled with the detector chamber. The gas flow lines for the different circulation modes are indicated by red-dotted arrow lines.

In the present work, the effects of gas ageing and the efficiency of the gas-filter unit were investigated by performing measurements in close-loop circulation mode with and without filter. The filters used in the present study are "Gatekeeper GPU gas purifiers" which are regenerable and operates without heating and power supply [10]. According to their specifications, they remove O_2, H_2O, CO and CO_2 contaminants with outlet purity of <100 pptV. The operating temperature of the filter is between 0°C and 65°C. The maximum flow rate depends on the size of the filter cartridge. A one year life time of the filter is marked off with 1 ppm O_2 and 1 ppm H_2O inlet at maximum flow rate. Before carrying out any measurement, the detector chamber and the gas lines were cleaned by pumping the system upto a vacuum level of $\approx 3\times10^{-4}$ mbar. Several test measurements were performed with different flow rate, 50-300 sccm (standard cubic centimeters per minute) and a flow rate of 300 sccm was chosen for the measurements in this work.

Leak detection tests were performed by monitoring the pressure rise in volumes maintained at pressures lower than the atmospheric one, specifically the chamber on one side and the circulation pump on the other. The respective leak rates were estimated to be about 1.0×10^{-5} mbar.l/s and 2.4×10^{-5} mbar.l/s. To quantify the air (mainly N_2 and O_2) pollution due to these leaks, it is necessary to estimate the total gas amount enclosed in the system. A volume of 20 liter at 85 mbar was estimated for the chamber side while a volume of 6 liter at 1 bar was estimated for the pump, the gas vessel and the filter/by-pass lines before the valve for pressure regulation. Thus, one can consider a pollution of about 0.15 % and 0.20 % of air over 100 h in circulation modes and static mode respectively. However, as already mentioned, these pollution rates are based on the total gas volume, that is different depending on the circulation and filter types. The gas volume (at 1 bar) is approximately 1 liter more in circulation mode without a filter because of the bypass line (see Figure 2). In circulation mode with filter, the volume will also vary depending on the size of the filter.

3. Data analysis methodology

To study the effects of gas ageing on the detector performance over time and compare the effects in different gas conditions, the total charge (which is proportional to the energy deposit) and the range of α-particles in Mayaito detector were measured. The accumulation of contaminants in the gas will affect gain and stopping power, thus changing the charge and range values, respectively. Measurements were performed for long run periods (several days) and the data were analyzed in interval of one hour duration over the entire run period. Data analysis was performed by using macros developed in the framework of ROOT analysis package [11]. Calibration of the Gassiplex channels was performed by sending pulser signals of different amplitudes to the anode. In Figure 3(a), energy loss of α-particles is reported as a function of pad number, showing a typical Bragg's curve. To generate a clean Bragg's curve and extract the correct information on energy and stopping point it is necessary to remove events generated by alpha particles emitted with larger angle that do not stop in the active region. Such events are characterized by short ionization tracks and partial energy loss in the gas volume. Only events whose stopping point is within 3σ of the stopping point distribution were then considered in the analysis. In order to be more selective on the particle track topology and to obtain better resolution, a second gating condition was applied. This condition, applied to only 4 pads, required keeping only the events for which the charge induced in these pads fall within 3σ of their corresponding charge distribution. Figure 3(b) shows the Bragg's curve obtained after applying the described conditions. The stopping point (SP) corresponds to a pad in which the value of charge

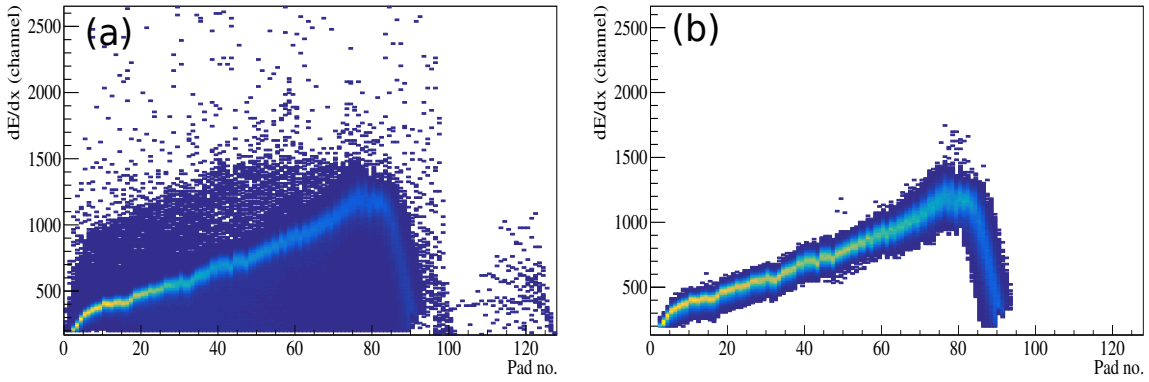

Figure 3: Bragg's curve of α-particles (a) before and (b) after applying gates (see text for details).

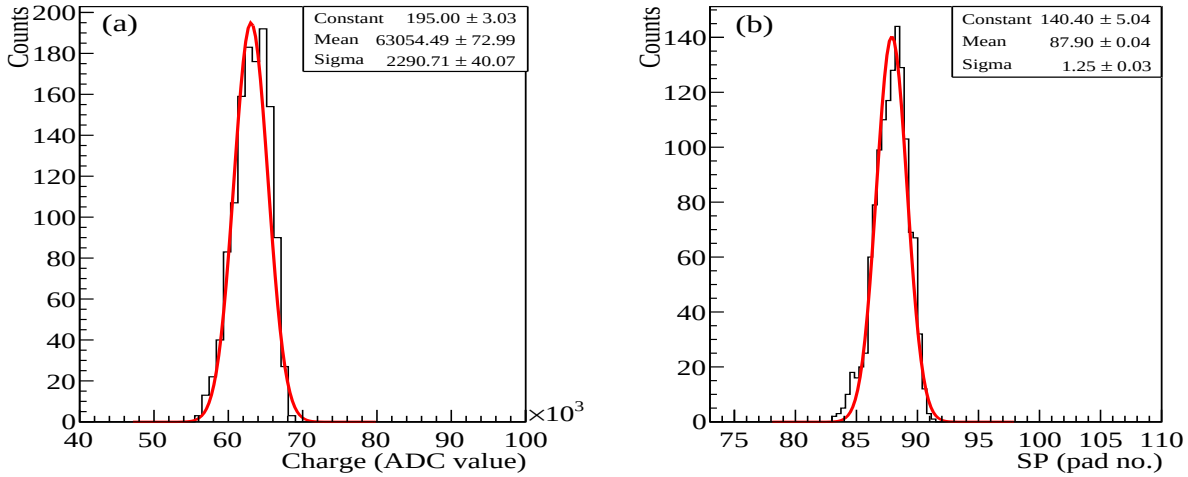

Figure 4: (a) Energy (through total charge measurement) and (b) Stopping point (SP) distributions of α-particles. The red curves are the results of Gaussian fit and the fit parameters are shown in the figure inset.

deposited is half of the value at the Bragg's peak. It was determined by performing a cubic spline interpolation of the Bragg's curve [12]. This pad number associated with the SP of the α-particle is referred to as the Last-pad.

The total charge was calculated by summing the ADC values of each pad from the First-pad to the Last-pad, thus giving at the end a value proportional to the energy deposit in the active volume and the gain. Figure 4 shows the charge and SP distributions of alpha particles over 1 hour duration. Mean charge and SP values are extracted by performing Gaussian fit in the distribution plots as shown in the figure. The errors in charge and SP are the errors in the corresponding mean value. The resolution was calculated from the ratio of the sigma (σ) and mean of the charge distribution.

4. Detector response and temperature dependence

Since, in gas-filled detector, the influence of environmental factors (temperature and pressure) on detector performance is well known [13], dedicated measurements were performed to investigate this kind of dependencies. As an example, in Figure 5 and 6, the charge, its resolution and SP were plotted as a function of time for static and circulation mode (with filter) respectively. In these figures, the temperature is also reported to highlight the real temperature variation during the measurement and to look into any possible correlation between them. In both static and circulation mode, the measured charge presents an oscillation pattern which correlates with the temperature variation during the run period. A similar correlation with temperature is observed in the SP in the case of circulation mode. While in the static mode, there is no significant change in the SP. In the resolution plots, which are shown in Figures 5(c) and 6(c), no considerable change was observed in both modes. Since the resolution does not show any variation attributable to the gas properties, this observable will not be considered further in this work. Attention will be focused on charge and SP. Variation in detector response with temperature can be due to temperature variation effect of the electronic components in the detector set-up (mainly Gassiplex) as well as gas condition variation inside the chamber. In order to study the change in detector response due to gas quality deterioration, it is necessary to understand and rectify the oscillation pattern observed in the measured value.

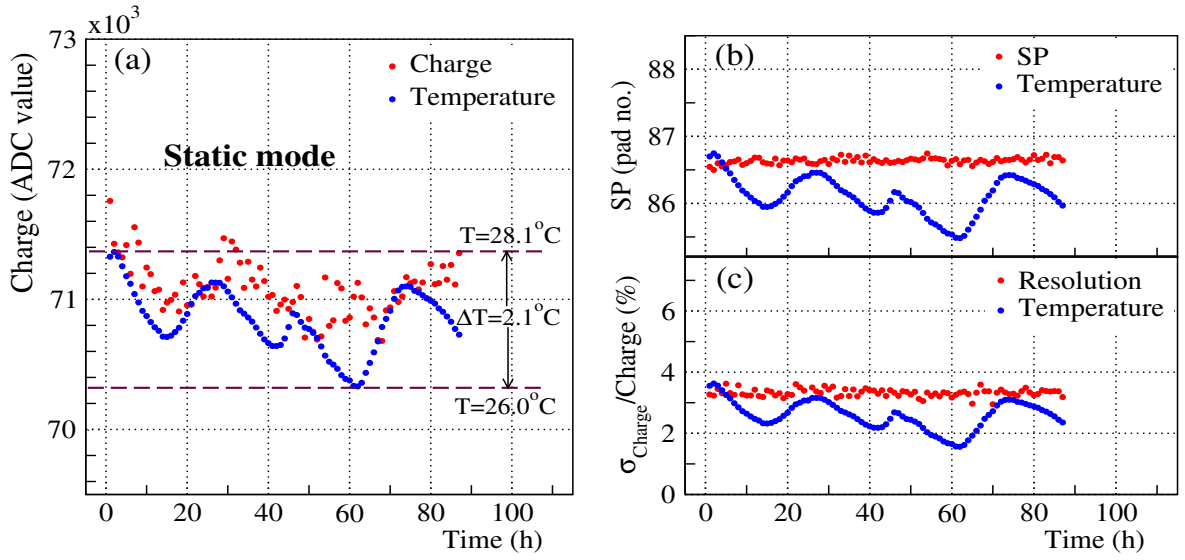

Figure 5: α-particles (a) total charge (b) stopping point and (c) resolution as a function of time measured in iC$_4$H$_{10}$ at 85 mbar in static mode. The temperature measured during the run is also reported.

5. Correction for temperature dependence in detector response

The effect of temperature variation on Gassiplex performance was retraced by sending a pulser signal to the Gassiplex through the Frisch's grid, which was then acquired in NUMEXO2 along with the α signal. Simultaneously, any possible pulser height variation during a measurement was also monitored by sending the same pulser signal directly to the NUMEXO2 digitizer. In order to understand the correlation between the variation of temperature and other signals, the ratio of the measured values of all the signals for each time slice t, $U(t)$, and their respective first measured values, U_0 (at t=1 h), were calculated. In Figure 7 the normalized signals of the measurement reported in Figure 6 are plotted as a function of time together with the Gassiplex-pulser and the Numexo-pulser signals. Oscillation pattern can be observed also for the Gassiplex-pulser and the Numexo-pulser,

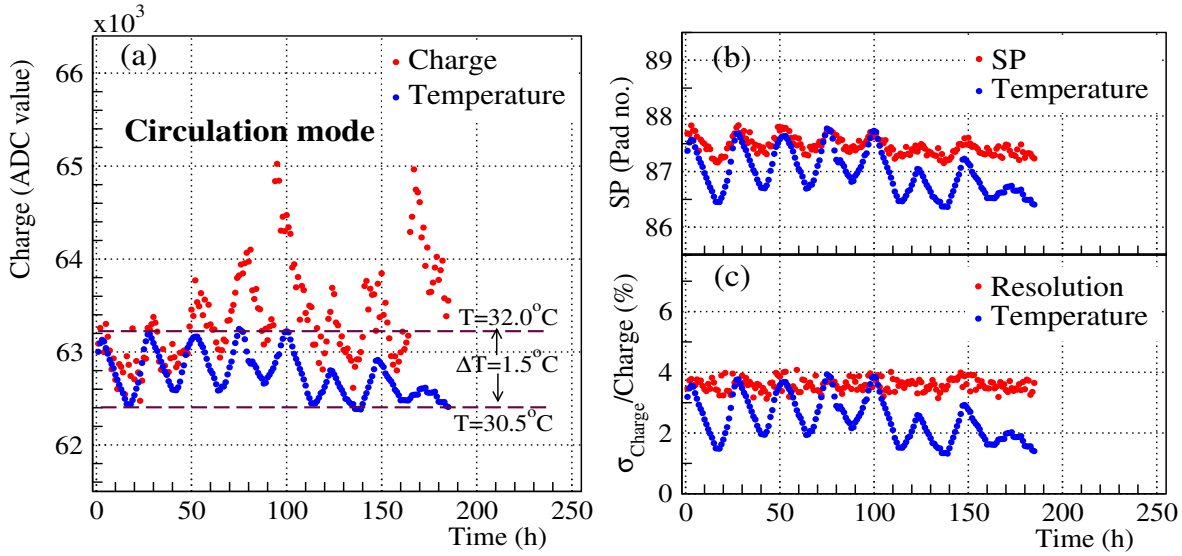

Figure 6: α-particles (a) total charge (b) stopping point and (c) resolution as a function of time measured in iC_4H_{10} at 85 mbar in circulation mode (with filter). The temperature measured during the run is also reported.

showing the possible temperature dependence of these signals. In order to make a fair comparison between detector performance under different gas conditions and look into the gas ageing effect, corrections have been applied in the data analysis to eliminate the temperature dependence. The following correction was applied:

1. Baseline corrections were applied to mean charges of the alpha and pulser (Gassiplex-pulser and Numexo-pulser) .
2. Correction in Gassiplex-pulser mean charge with respect to Numexo-pulser mean charge was applied to take care of pulser amplitude variation during a measurement.
3. Correction in charge with respect to Gassiplex-pulser was applied to deal with the temperature dependence of Gassiplex performance.

Correction factor for points (2) and (3) were calculated for each time slice by observing the deviation from the initial value. The plot of normalized charge after applying correction for variation in Gassiplex performance is shown in Figure 7 (black-dots) and it indicates a clear correlation between charge and temperature. A possible cause of such correlation is the variation in gas density inside the detector chamber due to the temperature variation. When the chamber is operated in circulation mode by regulating the pressure to a fixed value, a temperature variation implies a change in gas density inside the detector chamber according to the general gas equation. This hypothesis is supported by the observation that, when the Gassiplex correction is applied for charge measured in static mode (gas density is fixed) the correction cancels out the oscillation pattern. Moreover, as the gas density is fixed in static mode the SP is not sensitive to the temperature variation as can be observed in Figure 5(b).

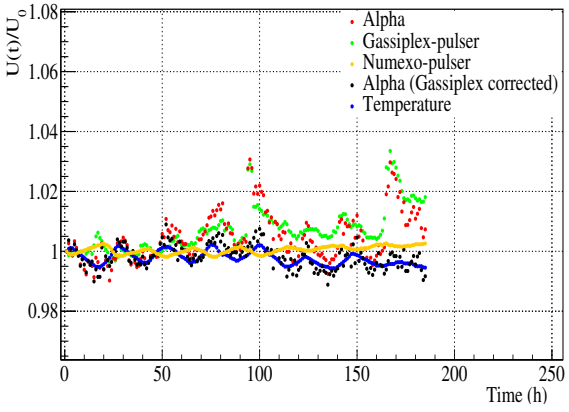

Figure 7: Ratio between measured signals at time t and their respective first values (at t=1 h) as a function of time (circulation mode with filter). Red-dots represent the alpha, green-dots the Gassiplex-pulser, yellow-dots the Numexo-pulser and the blue-dots the temperature. Black-dots represent the alpha signal after applying correction for variation in Gassiplex performance (see text for details).

Since, a minimal temperature variation is always present during a measurement, in the case of operation in circulation mode additional corrections were applied in the charge to take into account the density variation effect due to temperature. There are two possible consequences of density variation: (*i*) different energy lost in the dead zone (E_{DZ}) of the detector set-up and (*ii*) different detector gain. The correction for the E_{DZ} variation was

obtained by running SRIM simulation [14] for different densities of iC_4H_{10}. To obtain a correction factor for temperature-induced gain variation, a dedicated measurement of 3 h was performed by intentionally introducing a significant temperature variation. Due to the short duration of the run, the change in charge can be attributed only to temperature variation, while the impact of gas degradation is expected to be negligible. In Figures 8, 10, 12 and 14 the measured and corrected charge are reported. It has been observed that in circulation mode, the SP also fluctuates following the temperature variation. Thus, correction has been applied to take into account this dependence. The correction factor is the ratio of temperature at a given time t and the initial temperature value. As it is possible to see in Figure 11, 13 and 15 this correction removed out the oscillation pattern in the SP plots.

6. Ageing effects: results and discussions

In the present section measurements of charge and SP, corrected for the temperature dependence, are reported as a function of time for three different gas configurations: static mode, close-loop circulation (with and without filter) modes. In the close-loop circulation modes, 100% of the gas is recirculated i.e. no fresh gas is injected into the system. Once it is corrected, the electronics and temperature effects using the procedure described in the previous section, any variation of the charge and SP would be ascribed due to the accumulation of impurities in the gas. To quantify this variation, a linear fit of the data has been performed both on the charge and the SP data. The slope of the fit will provide the gas degradation rate in different operational modes.

6.1. Static mode

Figure 8 and 9 show the results of a measurement in static mode for charge and SP respectively. This measurement was performed to get a reference of the detector performance to compare with the measurements in close-loop circulation mode of the gas system. Considering the slope of the linear fit, a small degradation of 0.376±0.017 % per 100 h is observed for the gain with an increase of 0.023±0.005 % of the SP in the same time, meaning that the gain is more sensible to gas degradation than SP. Concerning the SP behaviour, a decrease of 0.15 % (250 μm) was expected due to the increasing gas pressure of about 0.2 % per 100 h, as discussed in Section 2. However, such a decrease is not seen in the data reported in the Figure 9, probably because of other effects (like, for instance, molecular adsorption) taking place when the pressure is not regulated. It can be assumed that the degradation in gain is due to contamination of mainly O_2 and H_2O molecules, whose presence would be responsible for electron attachment either in the drift region or in the amplification gap.

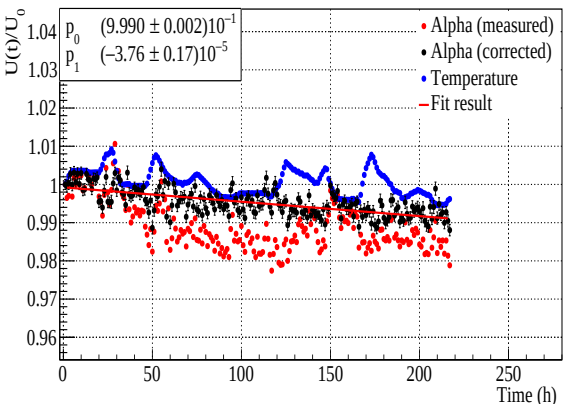

Figure 8: Normalized measured (red-dots) and corrected (black-dots) charge as a function of time. p_0 and p_1 in the inset are the intercept and the slope of the linear fit. Blue-dots are the normalized temperature (static mode).

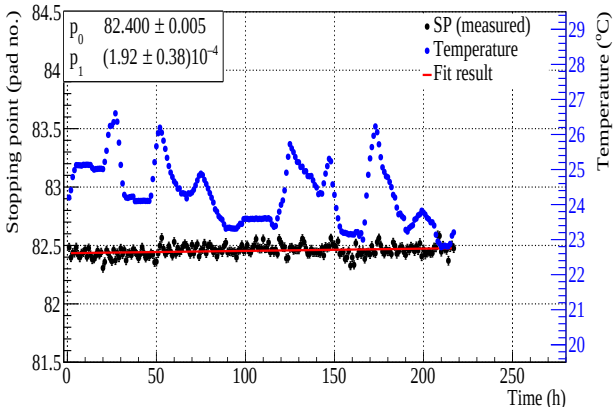

Figure 9: Measured stopping point (black-dots) as a function of time. p_0 and p_1 in the inset are the intercept and the slope of the linear fit. Blue-dots are the measured temperature (static mode).

6.2. Close-loop circulation mode without filter

The results for measurements of charge and SP in close-loop circulation without filter are shown in Figure 10 and 11 respectively. A larger gain degradation 0.74±0.03 % per 100 h) was observed as compare to the degradation in static mode although the air pollution has been estimated to be very similar in the two cases. Differently from static mode where the iC_4H_{10} amount remains constant, in circulation mode, pressure is regulated and air molecules will displace iC_4H_{10}. As a result, the fraction of O_2 and H_2O will increase and consequently the probability of electron attachment will be more important compared to the static mode.

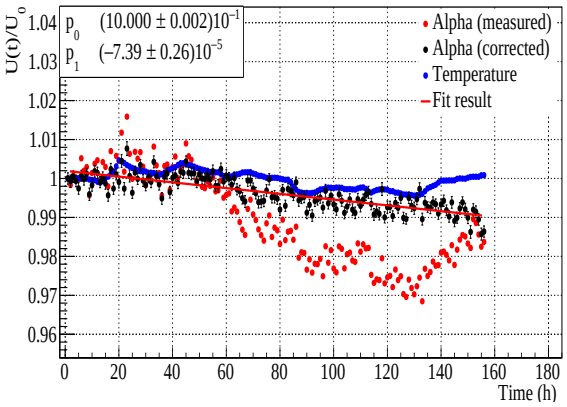

Figure 10: Normalized measured (red-dots) and corrected (black-dots) charge as a function of time. p_0 and p_1 in the inset are the intercept and the slope of the linear fit. Blue-dots are the normalized temperature (circulation mode without filter).

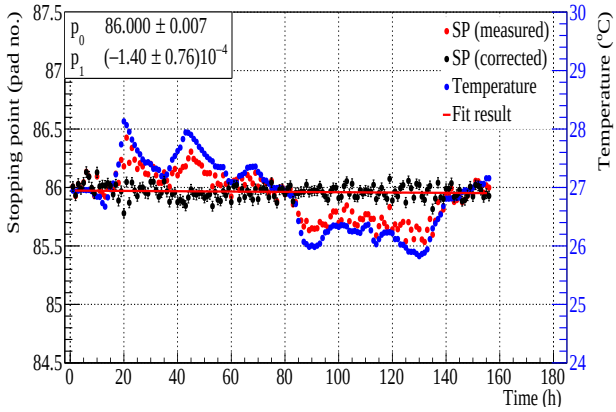

Figure 11: Measured (red-dots) and corrected (black-dots) stopping point as a function of time. p_0 and p_1 in the inset are the intercept and the slope of the linear fit. Blue-dots are the measured temperature (circulation mode without filter).

The SP variation is of about 0.016±0.009 % confirming that the leak rate is not important and therefore, demonstrates the proper functionality of the detector and the gas system set-up. In fact, a significant leakage will consequence to a notable change in the SP, as observed in [15]. On the other hand, this run was done for 156 h, which is not long enough to see an obvious change in the SP. For this reason, the runs in circulation mode with filter, detailed in the next section, were performed with longer run time.

6.3. Close-loop circulation mode with filter

In the case of circulation mode with filter, considering the small leakage rates and the filters capabilities, one could expect that O_2 and H_2O molecules are not present anymore in the chamber. Seperate measurements were performed under same conditions (flow rate and pressure) using two different filters of similar type but of different size which support different maximum flow rate: 20 slpm (standard liter per minute) and 1 slpm. The results are shown in Figure 12 - 15 for both the cases.

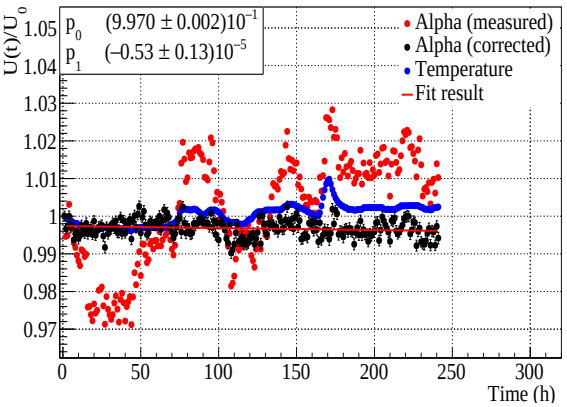

Figure 12: Normalized measured (red-dots) and corrected (black-dots) charge as a function of time. p_0 and p_1 in the inset are the intercept and the slope of the linear fit. Blue-dots are the normalized temperature (circulation mode with filter, 20 slpm).

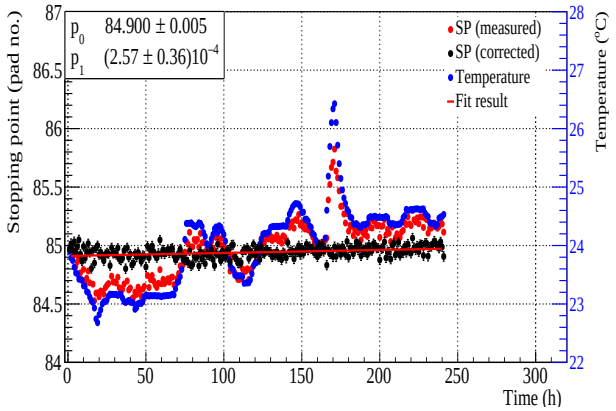

Figure 13: Measured (red-dots) and corrected (black-dots) stopping point as a function of time. p_0 and p_1 in the inset are the intercept and the slope of the linear fit. Blue-dots are the measured temperature (Circulation mode with filter, 20 slpm).

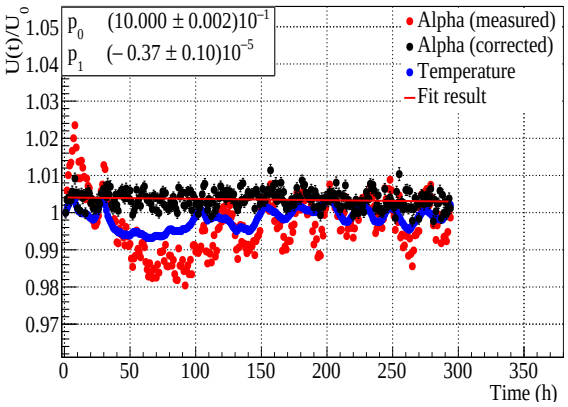

Figure 14: Normalized measured (red-dots) and corrected (black-dots) charge as a function of time. p_0 and p_1 in the inset are the intercept and the slope of the linear fit. Blue-dots are the normalized temperature (circulation mode with filter, 1 slpm).

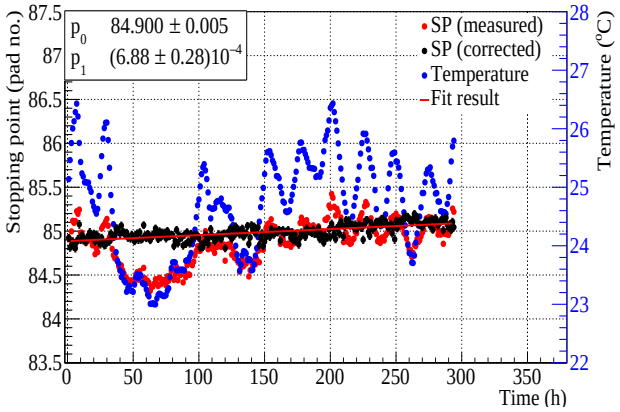

Figure 15: Measured (red-dots) and corrected (black-dots) stopping point as a function of time. p_0 and p_1 in the inset are the intercept and the slope of the linear fit. Blue-dots are the measured temperature (Circulation mode with filter, 1 slpm).

Degradation of the gain is negligible (about 0.05±0.01 % per 100 h with the 20 slpm filter and about 0.04±0.01 % per 100 h with the 1 slpm filter) if compared to the one observed in static and circulation mode without filter, confirming the idea that the charge degradation observed in the previous configurations could be due to electron attachment in O_2 and H_2O molecules. Since the filter used in the present study is not adapted for N_2 removal, there is possibility of N_2 accumulation with progressing run time due to the small leakage in the system. While it is not significant to deteriorate the detector gain, it is possible that the regular SP increase of 0.030±0.004 % (50 μm) and 0.081±0.003 % (125 μm) per 100 h with the 20 slpm and 1 slpm filters respectively would be attributable to the N_2 accumulation. As already mentioned, the total gas volume is higher with the bigger filter and hence the influence of leak on the SP is smaller. These SP increases are somehow consistent with the leakage rate (about 0.15 % per 100 h), since one can wait for a SP increase of 150 μm every 100 h.

7. Conclusion

In the framework of ACTAR-TPC, a gas system in close-loop that integrates a gas filtering unit was developed. The study was performed by measuring the response of Mayaito detector to α-particles, in terms of gain and stopping point. Considering the low energy beams available at GANIL, ACTAR-TPC is usually operated below atmospheric pressure, this R&D was thus performed at a low pressure of 85 mbar of isobutane. After applying all the necessary corrections of electronics response and density variations due to temperature, it has been demonstrated that working in close-loop with a gas filtering unit online is achievable, as long as the detector chamber is of course clean and the leakage rate is minimized. The gas-filter permits to maintain an optimal purity level of the gas and to re-inject it into the chamber in order to minimize the gas losses. A stable gain operation of more than 10 days was achieved (charge measurement stability of 0.12±0.02 %), which confirms the suitability of the system for ACTAR-TPC experiments. This marks an advance towards the objective of accessing nuclear physics experiment with expensive gases (specially isotopic gases like ^{3}He) in a near future with ACTAR-TPC at GANIL. A new study will be conducted to enhance the gas system, aiming to filter out the N_2 as well and retaining the isotopic gas purity as much as possible. It is worth noting that the utilization of isotopic gas forbid the use of additional gas like quenchers in order to keep them pure and to re-use the gas for several experiments. An upgrade in the amplification technique of ACTAR-TPC will be essential to address limitations in gain and sparking voltages associated with pure isotopic gas.

Acknowledgement

The financial assistance provided by the grant "RIN Recherche ACTARGP 21E04801 is acknowledged. We are grateful to A. Giret, G. Frémont, J. Goupil, C. Houarner, M. Prieur and F. Saillant of Grand Accélérateur National d'Ions Lourds, CEA/DRF-CNRS/IN2P3, B.P. 55027, Caen, Cedex, France., and O. Guillaudin of Laboratoire de Physique Subatomique & Cosmologie, 38000, Grenoble, France for their help and support in carrying out the study.

References

[1] B. Mauss, et al., Commissioning of the ACtive TARget and Time Projection Chamber (ACTAR TPC), Nucl. Instrum. Methods Phys. Res. A 940 (2019) 498.

[2] J. Giovinazzo, et al., 4D-imaging of drip-line radioactivity by detecting proton emission from ^{54m}Ni pictured with ACTAR TPC, Nat. Commun. 12 (2021) 4805.

[3] E. C. Pollacco, et al., GET: A generic electronics system for TPCs and nuclear physics instrumentation, Nucl. Instrum. Methods Phys. Res. A 887 (2018) 81–93.

[4] J. Giovinazzo, et al., ACTAR TPC performance with GET electronics, Nucl. Instrum. Methods Phys. Res. A 953 (2020) 163184.

[5] S. Frauendorf, A. Macchiavelli, Overview of neutron-proton pairing, Prog. in Part. and Nucl. Phys. 78 (2014) 24.

[6] R. Guida, B. Mandelli, A portable gas recirculation unit for gaseous detectors, JINST 12 (2017) T10002.

[7] M. Capeans, et al., RPC performances and gas quality in a closed loop gas system for the new purifiers configuration at LHC experiments, JINST 8 (2013) T08003.

[8] L. Gaudefroy, G. Mukherjee, F. Rejmund, Report on the range and stopping power measurements of ions in gases performed at GANIL: A part of R & D for the ACTAR project, GANIL internal report (2006).

[9] J.-C. Santiard, et al., Gasplex: a low-noise analog signal processor for readout of gaseous detectors, CERN-ECP-94-17 (1994).

[10] Entegris, GateKeeper® GPU HX Media Gas Purifiers (GPUS200FIX04R02C, GPUS35FIX04R02), `https://www.entegris.com/content/dam/product-assets/gatekeepergpugaspurifiers/datasheet-gatekeeper-gpu-hx-media-gas-purifiers-10962.pdf`.

[11] R. Brun, F. Rademakers, ROOT - An Object-Oriented Data Analysis Framework, Nucl. Instrum. Methods Phys. Res. A 389 (1997) 81–86.

[12] T. Roger, et al., Tracking algorithms for the active target MAYA, Nucl. Instrum. Methods Phys. Res. A 638 (2011) 134.

[13] L. Benussi, et al., Sensitivity and environmental response of the CMS RPC Gas Gain Monitoring system, JINST 4 (08) (2009) P08006.

[14] J. F. Ziegler, M. Ziegler, J. Biersack, SRIM – the stopping and range of ions in matter, Nucl. Instrum. Methods Phys. Res. A 268 (2010) 1818–1823.

[15] K. Rojeeta Devi, et al., Impact of gas degradation on Mayaito detector performance, submitted to Proceedings of the 3rd International Conference on Detector Stability and Aging Phenomena in Gaseous Detectors, Nucl. Instrum. Methods Phys. Res. A (2024).